Estimation of Linear Shape Deformations and its Medical Applications

Zoltan Kato, Attila Tanács, and Csaba Domokos

Abstract

In this report, we present the main results of our work supported by the OTKA K-75637 grant during January 2009 – March 2012. The main achievement of the project is a *fully functional automatic shape registration method* with the following properties:

- it doesn't need established point correspondences nor the use of iterative optimization algorithms;
- capable of recovering 2D linear and (invertible) projective shape deformations as well as affine distortions of 3D shapes;
- robust in the presence of geometric noise and various segmentation errors;
- has a linear time complexity allowing near real-time registration of high resolution images.

We made publicly available three demo programs implementing our affine 2D, 3D and planar homography registration algorithms. Furthermore, we have also developed a prototype software for aligning hip prosthesis X-ray images, which has been transfered to collaborating radiologists for further exploitation and validation for potential application in everyday health care.

Our results have been presented at top conferences of the field (*e.g. ICCV*, *ECCV*) as well as in leading journals (*e.g. IEEE Transactions on Pattern Analysis and Machine Intelligence*, *Pattern Recognition*). One of the MSc students working on the project received the second price of the *National Scientific Student Conference* (*OTDK*). Csaba Domokos successfully defended his PhD degree (*Summa cum laude*) and his work on solving *affine puzzle*s has been awarded the prestigious *Attila Kuba Prize* of the *Hungarian Association for Image Processing and Pattern Recognition*. More details about our results can be found at the project's webpages:

- http://www.inf.u-szeged.hu/ipcg/projects/AFFSHAPE.html
- http://www.inf.u-szeged.hu/ipcg/projects/AffinePuzzle.html
- http://www.inf.u-szeged.hu/ipcg/projects/diffeoshape.html

I. PROBLEM STATEMENT AND PROPOSED APPROACH

In this project, we considered the estimation of linear transformations aligning a known binary shape and its distorted observation. The classical way to solve this registration problem is to find correspondences between the two images and then compute the transformation parameters from these landmarks. We developed a unified framework where the exact transformation is obtained as the solution of either a polynomial or a linear system of equations without establishing correspondences. The advantages of the proposed solutions are that they are fast, easy to implement, have linear time complexity, work without landmark correspondences and are independent of the magnitude of transformation.

Let us denote the points of the *template* and the *observation* by $\mathbf{x}, \mathbf{y} \in \mathbb{P}^2$ respectively (*i.e.* we use homogeneous coordinates). $\mathbf{A}$ is the unknown non-singular linear transformation that we want to recover. We can define the identity relation as follows

$$\mathbf{A}\mathbf{x} = \mathbf{y} \quad \Leftrightarrow \quad \mathbf{x} = \mathbf{A}^{-1}\mathbf{y}. \tag{1}$$

If we can observe some image features (*e.g.* gray-level of the pixels) that are invariant under the transformation $\mathbf{A}$ then the following equality also holds

$$g(\mathbf{x}) = h(\mathbf{A}\mathbf{x}) \quad \Leftrightarrow \quad g(\mathbf{A}^{-1}\mathbf{y}) = h(\mathbf{y}). \tag{2}$$

Furthermore, the above equations still hold when an *invariant function* $\omega : \mathbb{R}^n \to \mathbb{R}^n$ is acting on both sides of the equations. Indeed, for a properly chosen ω

$$\omega(\mathbf{x}) \;=\; \omega(\mathbf{A}^{-1}\mathbf{y}), \quad \text{and} \tag{3}$$

$$\omega(g(\mathbf{x})) \;=\; \omega(h(\mathbf{A}\mathbf{x})) = \omega(h(\mathbf{y})). \tag{4}$$

The basic idea of the proposed approach is to generate enough linearly independent equations by making use of the relations in Eq. (1)–(4). Furthermore, we can get rid of the need for point correspondences by integrating both sides of the equations over the corresponding segmented domains.

The main challenge of the proposed approach is to find a way to construct a direct method to estimate linear deformations without making use of feature correspondences or complex optimization algorithms. In this project, we propose two ways to tackle this fundamental problem.

II. SOLUTION VIA A POLYNOMIAL SYSTEM

The first one [1], [3] makes use of Eq. (3) and constructs a system of polynomial equations

$$\int \omega(\mathbf{x})d\mathbf{x} = \frac{1}{|\mathbf{A}|} \int \omega(\mathbf{A}^{-1}\mathbf{y})d\mathbf{y}. \tag{5}$$

Obviously, the choice of ωs is crucial as our goal is to construct a system which can be solved. It is easy to see that a polynomial system, which is certainly straightforward to solve, is obtained when $\omega(x) = x^i$. From a geometric point of view, for $\omega(x) \equiv x$ Eq. (5) simply matches the center of mass of the *template* and *observation* while for $\omega(\mathbf{x}) = [x_1^i, x_2^i, 1]^T$ Eq. (5) matches the center of mass of the shapes obtained by the nonlinear transformations ω. In the 2D affine case, we have to solve a system of polynomial equations of the following form, where q_{ki} denotes the unknown elements of the inverse transformation $\mathbf{A}^{-1}$

$$|\mathbf{A}| \int x_k = q_{k1} \int y_1 + q_{k2} \int y_2 + q_{k3} \int 1, \tag{6}$$

$$|\mathbf{A}| \int x_k^2 = q_{k1}^2 \int y_1^2 + q_{k2}^2 \int y_2^2 + q_{k3}^2 \int 1 + 2q_{k1}q_{k2} \int y_1 y_2 + 2q_{k1}q_{k3} \int y_1 + 2q_{k2}q_{k3} \int y_2, \tag{7}$$

$$|\mathbf{A}| \int x_k^3 = q_{k1}^3 \int y_1^3 + q_{k2}^3 \int y_2^3 + q_{k3}^3 \int 1 + 3q_{k1}^2 q_{k2} \int y_1^2 y_2 + 3q_{k1}^2 q_{k3} \int y_1^2 + 3q_{k2}^2 q_{k3} \int y_2^2$$
$$+ 3q_{k1}q_{k2}^2 \int y_1 y_2^2 + 3q_{k2}q_{k3}^2 \int y_2 + 3q_{k1}q_{k3}^2 \int y_1 + 6q_{k1}q_{k2}q_{k3} \int y_1 y_2. \tag{8}$$

The above system of equations can be readily solved either by a direct solver found *e.g.* in Matlab [1] or by a classical LSE solver like the *Levenberg-Marquardt* algorithm [2].

A. Registration of 3D Objects

The extension of the polynomial method to 3D objects [2]–[4] is relatively straightforward. However, numerical implementation has to be carefully designed. Therefore, both in 2D and 3D we examined two different types of solution methods: iterative least-squares solutions and direct analytical solutions.

- In case of a direct method, limited number of equations can be used (according to the degree of freedom of the n-dimensional affine transformation), while an iterative approach allows for an overdetermined system, which may give more stability.
- Direct methods may provide many hundreds or even thousands of possible solutions, many (or even all) of them may be complex thus a solution selection scheme has to be used to produce only one real solution from these. Iterative methods can provide only one real solution, but the search may fall into local minima. To avoid such local minima, usually a sophisticated search strategy is necessary.
- Direct methods can provide full affine solutions only, in case of iterative methods restrictions to lower degree of freedom transformations are easy to impose.

We found that the direct approach gives more stable results, but the iterative one is more precise. It is also possible to combine the two approaches: The direct approach provides the initialization of the iterative one.

Another issue is discretization error, which might be particularly problematic in 3D. For that purpose, we extended our method by investigating the case when the segmentation method is capable of producing *fuzzy object*s instead of a binary result in both 2D and 3D. It has been shown that the information preserved by using fuzzy representation based on area coverage may be successfully utilized to improve precision and accuracy of our equations [2], [3]. The result of a series of synthetic tests showed that fuzzy representation yields lower registration errors in average.

B. Affine Puzzle

The affine puzzle problem can be formulated as follows: Given a binary image of an object (the template) and another binary image (the observation) containing the fragments of the template, we want to establish the geometric correspondence between these images which reconstructs the complete template object from its parts. The overall distortion is a global nonlinear transformation with the following constraint (see Fig. 3):
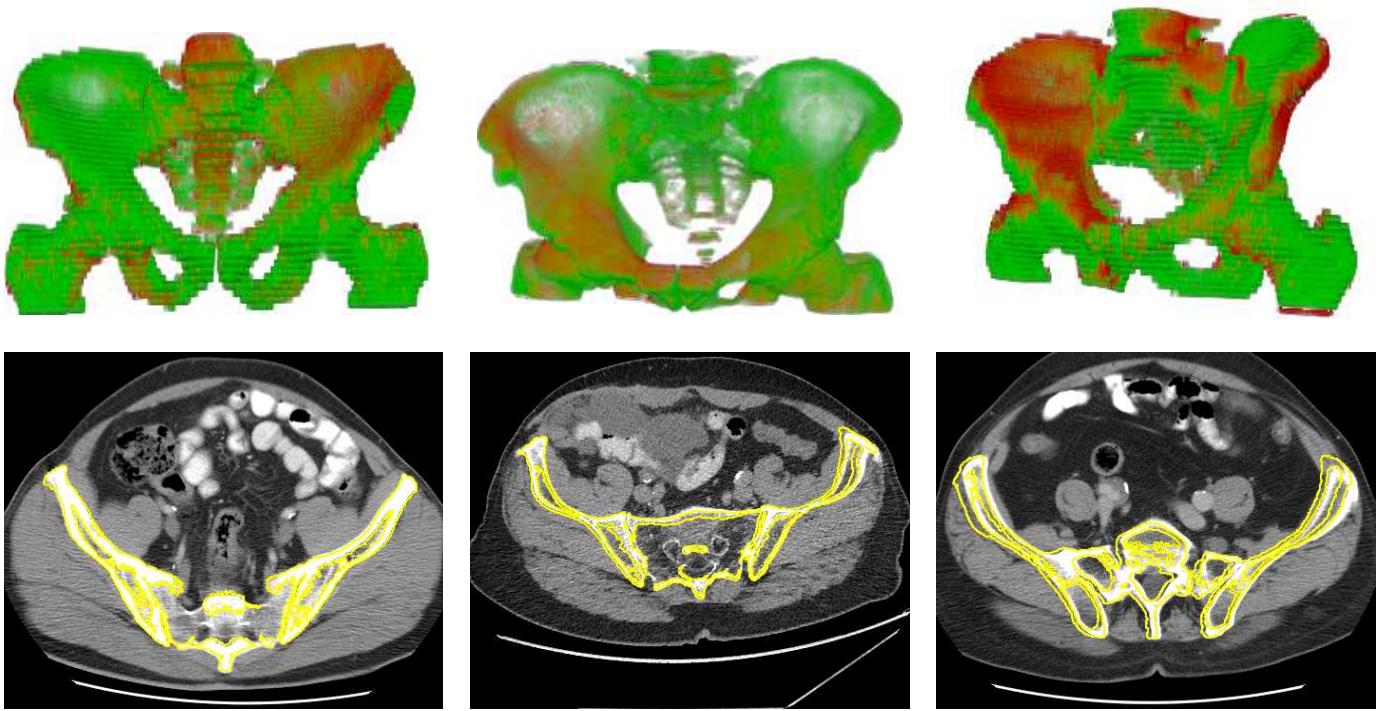
Fig. 1.   Registration of pelvic CT data: superimposed registered 3D bone models (top row), and bone contours of the registered template (yellow) overlayed on a CT slice of the observations (bottom row). δ errors are 14.2%, 19%, and 27.87%. The first two cases show good alignment. Even the third one can be regarded as a fast, coarse approximation.
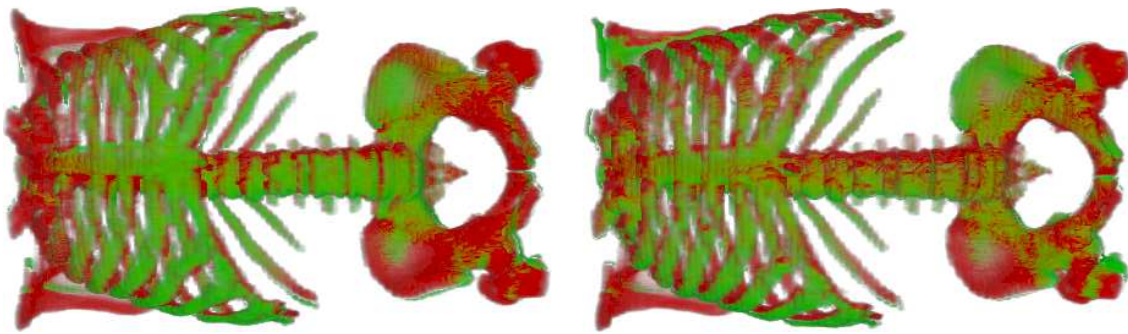

Fig. 2.   Registration of thoracic CT data: superimposed registered 3D bone models. Perfect alignment is not possible due to the relative movements of the bone structure. Affine alignment results are used as a good starting point for *e.g.* lymph node detection.

- the object parts are distinct (*i.e.* either disconnected or separated by segmentation),
- all fragments of the template are available, but
- each of them is subject to a different affine deformation, and the partitioning of the template object is unknown.

The proposed solution [5] consists in constructing and solving a polynomial system of equations similar to Eq. (6)–(8), which provides all the unknown parameters of the alignment. We have quantitatively evaluated the proposed algorithm on a large synthetic dataset containing 2D and 3D images. The results show that the method performs well and robust against segmentation errors. The method has been validated on 2D real images of a tangram puzzle (see Fig. 4) as well as on volumetric medical images applied to surgical planning (see Fig. 5).
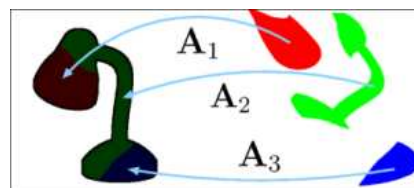

Fig. 3.   Affine puzzle: reconstructing the complete template object from its deformed parts.
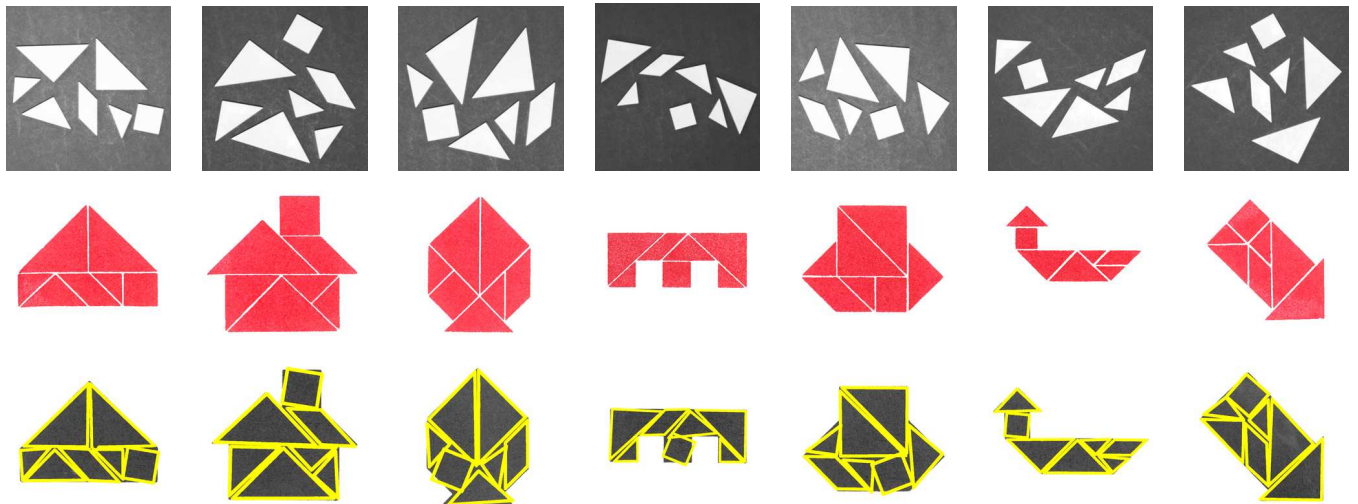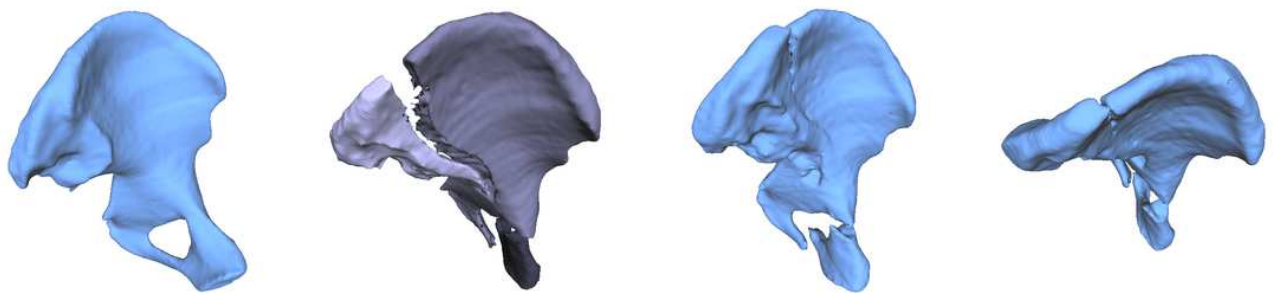
Fig. 4. Solutions of the Tangram puzzle (the average alignment runtime of an image was about 50 sec. in Matlab). **Top:** *Observations* are taken by digital camera. **Middle:** Solutions, found in the Tangram manual. **Bottom:** The scanned *template* silhouettes with overlaid contours of aligned fragments.

template obtained by mirroring intact bone

observation

realigned bone fragments

Fig. 5. Bone fracture reduction (CPU time in Matlab was 15 sec. for these 1 megavoxel CT volumes).

Fig. 6. Homography registration results on traffic signs. The first row shows the *template*s while below them the corresponding *observation*s with the overlaid contour of the registration results.

C. Planar Homography

Perspective images of planar scenes are usual in perception of man made environments. In such cases, a planar scene and its image are related by a plane to plane homography, also known as a plane projective transformation. Estimating the parameters of such transformations is a fundamental problem in computer vision with various applications.

Let us denote the homogeneous coordinates of the *template* and *observation* by $\mathbf{x}' = [x_1', x_2', x_3']^T \in \mathbb{P}^2$ and $\mathbf{y}' = [y_1', y_2', y_3']^T \in \mathbb{P}^2$, respectively. Planar homography is then a linear transformation in the projective plane $\mathbb{P}^2$

$$\mathbf{y}' = \mathbf{H}\mathbf{x}' \quad \Leftrightarrow \quad \mathbf{x}' = \mathbf{H}^{-1}\mathbf{y}' ,\tag{9}$$

where $\mathbf{H} = \{H_{ij}\}$ is the unknown 3×3 transformation matrix that we want to recover. As usual, the inhomogeneous coordinates $\mathbf{y} = [y_1, y_2]^T \in \mathbb{R}^2$ of a homogeneous point $\mathbf{y}'$ are obtained by projective division

$$
\begin{aligned}
y_1 &= \frac{y_1'}{y_3'} = \frac{H_{11}x_1 + H_{12}x_2 + H_{13}}{H_{31}x_1 + H_{32}x_2 + 1} \equiv \chi_1(\mathbf{x}) \\
y_2 &= \frac{y_2'}{y_3'} = \frac{H_{21}x_1 + H_{22}x_2 + H_{23}}{H_{31}x_1 + H_{32}x_2 + 1} \equiv \chi_2(\mathbf{x}) ,
\end{aligned}\tag{10}
$$

where $\chi_i : \mathbb{R}^2 \to \mathbb{R}$. Indeed, planar homography is a linear transformation in the projective plane $\mathbb{P}^2$, but it becomes nonlinear within the Euclidean plane $\mathbb{R}^2$. The nonlinear transformation corresponding to $\mathbf{H}$ is denoted by $\chi : \mathbb{R}^2 \to \mathbb{R}^2$, $\chi(\mathbf{x}) = [\chi_1(\mathbf{x}), \chi_2(\mathbf{x})]^T$ and the Jacobian determinant $|J_\chi| : \mathbb{R}^2 \to \mathbb{R}$ is given by

$$|J_\chi(\mathbf{x})| = \begin{vmatrix} \frac{\partial \chi_1}{\partial x_1} & \frac{\partial \chi_1}{\partial x_2} \\ \frac{\partial \chi_2}{\partial x_1} & \frac{\partial \chi_2}{\partial x_2} \end{vmatrix} = \frac{|\mathbf{H}|}{(H_{31}x_1 + H_{32}x_2 + 1)^3} ,\tag{11}$$

and Eq. (5) becomes

$$\int \omega(\mathbf{y})d\mathbf{y} = \int \omega\big(\chi(\mathbf{x})\big) |J_\chi(\mathbf{x})| \, d\mathbf{x}.\tag{12}$$

The resulting system of equations can be easily solved in the least squares sense by the Levenberg-Marquard algorithm [6], [7]. Some examples of traffic sign registration results are shown in Fig. 6.

III. SOLUTION VIA A LINEAR SYSTEM USING COVARIANT FUNCTIONS

The second solution to our 2D affine registration problem [8], [9] is based on Eq. (4). The advantage of this approach is that it yields a linear system of equations which is numerically much more stable. The key idea is to construct a *covariant function* pair satisfying Eq. (2). Once this is achieved, we can set up a linear system using Eq. (4) to solve for the unknown transformation $\mathbf{A}$. Since we do not have any radiometric information, this is a quite challenging task as we have to define these functions based on the only available geometric information. For example, we can consider the points of the *template* as a sample from a normally distributed random variable $X \sim N(\mu, \Sigma)$. It is well known, that for any linear transformation, when $Y = \mathbf{A}X$ then Y has also a normal distribution

$$X \mapsto Y \sim N(\mu', \Sigma') = N(\mathbf{A}\mu, \mathbf{A}\Sigma\mathbf{A}^T),\tag{13}$$

furthermore

$$p'(\mathbf{y}) = \frac{1}{|\mathbf{A}|}p(\mathbf{x}),\tag{14}$$

where p' and p are the Gaussian density functions. It is clear that p and p' are *covariant* and the Jacobian can also be computed as $|\mathbf{A}| = \sqrt{|\Sigma'|/|\Sigma|}$. Obviously, the above relation is only valid when $\mathbf{A}$ is positive definite. The parameters of the probability densities $N(\mu, \Sigma)$ and $N(\mu', \Sigma')$ can be easily estimated as the sample means and covariances (*i.e.* the mean and covariance of the point coordinates). From a geometric point of view, the mean values μ and μ' represent the center of mass of the *template* and *observation* respectively, while Σ and Σ' capture the orientation and eccentricity of the shapes. Note that the densities p' and p can be further reduced to the corresponding Mahalanobis distances g and h

$$g(\mathbf{x}) = (\mathbf{x} - \mu)^T\Sigma^{-1}(\mathbf{x} - \mu) \quad \text{and} \quad h(\mathbf{y}) = (\mathbf{y} - \mu')^T\Sigma'^{-1}(\mathbf{y} - \mu').\tag{15}$$

New equations can then be generated by making use of appropriate *invariant functions* $\omega : \mathbb{R} \to \mathbb{R}$. Thus we get

$$\int \mathbf{x}\omega(g(\mathbf{x}))d\mathbf{x} = \int \mathbf{x}\omega(h(\mathbf{A}\mathbf{x}))d\mathbf{x} = \frac{1}{|\mathbf{A}|} \int \mathbf{A}^{-1}\mathbf{y}\omega(h(\mathbf{y}))d\mathbf{y}.\tag{16}$$

	Runtime (sec.)	ϵ (pixel)	δ (%)
Polynomial	0.98	0.51	0.15
Linear	1.5	5.42	2.6
Mult. covar. functions	0.33	0.54	0.19

TABLE I

MEDIAN OF REGISTRATION ERRORS AND CPU TIMES ON A BENCHMARK DATASET OF SYNTHETIC PLANAR SHAPES.

Theoretically any *invariant function* could be applied. For example the following set of functions gave us good results [8]: x, $\cos(x)$, $\cos(2x)$, $\sin(x)$ and $\sin(2x)$ (see Fig. 8 for another function set). In the affine case, we can write the linear system in matrix form

$$\begin{pmatrix} \int y_1\omega_1(h(\mathbf{y})) & \int y_2\omega_1(h(\mathbf{y})) & \int \omega_1(h(\mathbf{y})) \\ \vdots & \vdots & \vdots \\ \int y_1\omega_n(h(\mathbf{y})) & \int y_2\omega_n(h(\mathbf{y})) & \int \omega_n(h(\mathbf{y})) \end{pmatrix} \begin{pmatrix} q_{k1} \\ q_{k2} \\ q_{k3} \end{pmatrix} = |\mathbf{A}| \begin{pmatrix} \int x_k\omega_1(g(\mathbf{x})) \\ \vdots \\ \int x_k\omega_n(g(\mathbf{x})) \end{pmatrix}. \quad (17)$$

The solution of the above linear system directly provides the parameters of the aligning transformation [8], [9].

A. Compound Objects

When we have objects composed of several parts, yielding a group of disjoint shapes when segmented, the topology of such compound shapes will not change under the action of the affine group. Thus we can construct covariant functions $\mathcal{P}_i(\mathbf{x})$, $\mathcal{S}_i(\mathbf{y})$ for each pair of these shape parts and then sum these relations yielding [9]

$$P(\mathbf{x}) \equiv \sum_{i=0}^{m} \mathcal{P}_i(\mathbf{x}) = \sum_{i=0}^{m} \mathcal{S}_i(\mathbf{y}) \equiv S(\mathbf{y}). \quad (18)$$

where $\mathcal{P}_i(\mathbf{x}) = \exp\left(-\frac{1}{2}(\mathbf{x}-\mu_i)^T\Sigma_i^{-1}(\mathbf{x}-\mu_i)\right)$ are unnormalized Gaussians.

The big advantage of this representation is that we can get rid of the segmented shape used as the integration domain in Eq. (16). A clear disadvantage of using the segmented shape itself as the domain [8] is that any segmentation error will inherently result in erroneous integrals causing misalignment. In the case of compound shapes, however, it is natural to chose one of the ellipses of the density fitted to the overall shape as the integration domain (see Fig. 9). An additional benefit is that these domains are analytical hence the computation of the integrals used as coefficients in Eq. (17) can be computed efficiently by a closed form formula.

IV. SEGMENTATION METHOD USED FOR MEDICAL APPLICATIONS

Traumatic hip replacement is a surgical procedure in which the hip joint is replaced by a prosthetic implant. In the short term post-operatively, infection is a major concern. An inflammatory process causes bone resorption and subsequent loosening or fracture often requiring revision surgery. Alignment of a hip prosthesis X-ray images (see Fig. 7 and Fig. 8) allows for assessing loosening by comparing a number of post-operative X-ray images taken over a period of time. Since one is looking for deformations of the bone surrounding the implant, alignment must be based on the implant as it is the only imaged part which is guaranteed to remain unchanged from one image to the other.

Fast rigid-body registration of bone structures (*e.g.* see Fig. 5) is important in image guided surgical planning in execution for registering pre-operative volumes to intra-operative ones.

Rigid registration of thoracic images (see Fig. 2) are also applicable for *e.g.* lymphoma detections and changes over time using PET-CT scanners. PET images delineate the uptake of the contrast agent in organs (lymph nodes), while the CT modality can be used for registration and morphological localization. Here non-rigid registrations are discouraged since these could change the size of the organs.

A common part of the above applications is the segmentation of bony structures (or the metallic prosthesis) from 2D X-ray and 3D CT images. We have developed segmentation techniques for extracting such image regions with both crisp [4] and fuzzy [2], [3] representations.

Fig. 7. Alignment of hip prosthesis X-ray images using a polynomial system of equations with ω functions $\{x, x^2, x^3\}$. Registration results are shown as an overlayed contour on the second image.
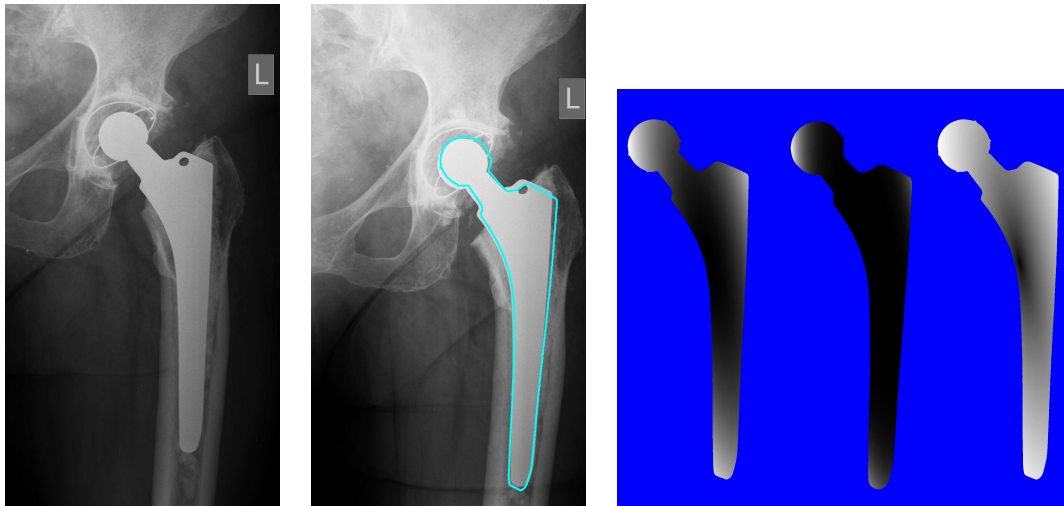

Fig. 8. Alignment of a hip prosthesis X-ray image using a linear system of equations with ω functions $\{x, x^3, x^{1/3}\}$. Registration result is shown as an overlayed contour on the second image.

V. COMPARISON OF THE TWO APPROACHES

The methods have been quantitatively evaluated on a set of more than 1000 synthetically generated observations for 60 different shapes. The applied affine transformations were randomly composed of $0°, 10°, \ldots, 350°$ rotations; $0, 0.4, \ldots, 1.2$ shearings; $0.5, 0.7, \ldots, 1.9$ scalings, and $-20, 0, 20$ translations along both axes. The resulting images are of size $\approx 1400 \times 1400$. For evaluation, we have computed two error measures: the Dice coefficient as $\delta = \frac{|R \triangle O|}{|R| + |O|} \cdot 100\%$, where $\triangle$ denotes symmetric difference, while T, R and O are the pixels of the *template*, *registered* object and *observation* respectively; and $\epsilon = \frac{1}{|T|} \sum_{\mathbf{p} \in T} \|(\mathbf{A} - \tilde{\mathbf{A}})\mathbf{p}\|$, which measures the average distance between the true $\mathbf{A}$ and the estimated $\tilde{\mathbf{A}}$ transformation. All algorithms were implemented in Matlab. These results are shown in Table I. Based on these numbers, it is clear that the polynomial solution provides rather good alignments at the price of $\approx 1\text{sec}$. CPU time. The linear system based on a single pair of covariant functions [8] given in Eq. (15) works well when there are no segmentation errors, but deteriorates quickly when pixels are missing. On the other hand, the linear system with multiple pairs of covariant functions given in Eq. (18) clearly outperforms the polynomial solution in terms of CPU time as well as in robustness: even for 90% missing pixels [9], this method still provides acceptable alignments while the polynomial system fails over 50% [1]. We also remark, that -like any other area based method- both approaches are quite sensitive to occlusions as it yields large errors in the system of equations.

In Fig. 7 and Fig. 8, we show registration results of hip prosthesys X-ray images. These results also confirm

Fig. 9.   Alignment of a traffic sign images using a linear system of equations with multiple shape parts. The first image shows the elliptic integration domain with the compound covariant function fitted over the *template*. Registration results are shown as an overlayed contour on the second image.

the higher precision of the polynomial system. While the multiple covariant function approach cannot be applied on these images since we only have a single shape, Fig. 9 shows the alignment of traffic signes where -due to the compound shape of these signs- the multiple covariant function approach works pretty well.

VI. DISSEMINATION AND FUTURE WORK

Our results have been published in
- two peer-reviewed international journals [1], [7],
- seven top tier peer-reviewed international conference proceedings [2]–[6], [9], [10],

The project's achievements have also been presented at leading international conferences

2009   International Conference on Computer Vision, International Conference on Image Processing, Scandinavian Conferences on Image Analysis.

2010   European Conference on Computer Vision, International Conference on Image Processing.

2011   International Conference on BioMedical Engineering and Informatics.

and national conferences:

2009,2011   Conference of the Hungarian Association for Image Analysis and Pattern Recognition.

Furthermore, Zoltan Kato gave keynote lectures about the project's results at the following international conferences:
- *International Conference on Signal Image Technology and Internet Based Systems (SITIS)*, November 2011, Dijon, France.
- *International Joint Conference on Computer Vision, Imaging and Computer Graphics Theory and Applications*, February 2012, Rome, Italy.

as well as invited talks at the following international research institutes:
- *Dept. Electronic Systems and Information Processing, University of Zagreb*, Zagreb, Croatia. May 2011
- *Center for Machine Perception, Czech Technical University*, Prague, Czech Republic. 8 November 2011.
- *Department of Image Processing, Institute of Information Theory and Automation of the ASCR*, Prague, Czech Republic. 11 November 2011.

Demo implementations of our most important algorithms are publicly available:

1) Affine Registration of Planar Shapes. JAVA code with a direct solver (only runs under Windows). Download from http://www.inf.u-szeged.hu/~kato/software/affbinregdemo.html

2) Affine Registration of 3D Objects. JAVA code with multi-threading (≈ 0.2 sec. CPU time for megavoxel volumes). Download from http://www.inf.u-szeged.hu/~kato/software/affbin3dregdemo.html

3) Nonlinear Shape Registration without Correspondences. JAVA code. Implements planar homography, extension to other nonlinear deformations is relatively easy. Download from http://www.inf.u-szeged.hu/~kato/software/planarhombinregdemo.html

The works of Jozsef Nemeth and Zsolt Katona MSc students have been presented at the *National Scientific Student Conference* (*OTDK*) in 2009, where Jozsef Nemeth obtained the second price. Csaba Domokos succesfully defended his PhD degree in 2011 [11] (*Summa cum laude*) and his work on solving the *affine puzzle* problem [5] has been awarded the prestigious *Attila Kuba Prize* of the *Hungarian Association for Image Processing and Pattern Recognition*.

A journal paper about the results presented in Section II-A is under review at *Pattern Recognition* [12]. Another journal paper about Gaussian covariants presented in Section III will be submitted to *Image and Vision Computing* [13].

REFERENCES

[1] C. Domokos and Z. Kato, "Parametric estimation of affine deformations of planar shapes," *Pattern Recognition*, vol. 43, no. 3, pp. 569–578, Mar. 2010.

[2] A. Tanács, N. Sladoje, J. Lindblad, and Z. Kato, "Estimation of linear deformations of 3D objects," in *Proceedings of International Conference on Image Processing*, IEEE. Hong Kong, China: IEEE, Sept. 2010, pp. 153–156.

[3] A. Tanács, C. Domokos, N. Sladoje, J. Lindblad, and Z. Kato, "Recovering affine deformations of fuzzy shapes," in *Proceedings of Scandinavian Conferences on Image Analysis*, ser. Lecture Notes in Computer Science, A.-B. Salberg, J. Y. Hardeberg, and R. Jenssen, Eds., vol. 5575. Oslo, Norway: Springer, June 2009, pp. 735–744.

[4] A. Tanacs and Z. Kato, "Fast linear registration of 3D objects segmented from medical images," in *Proceedings of International Conference on BioMedical Engineering and Informatics*. Shanghai, China: IEEE, Oct. 2011, pp. 299–303.

[5] C. Domokos and Z. Kato, "Affine puzzle: Realigning deformed object fragments without correspondences," in *Proceedings of European Conference on Computer Vision*, ser. Lecture Notes in Computer Science, K. Daniilidis, P. Maragos, and N. Paragios, Eds., vol. 6312. Crete, Greece: Springer, Sept. 2010, pp. 777–790.

[6] J. Nemeth, C. Domokos, and Z. Kato, "Recovering planar homographies between 2D shapes," in *Proceedings of International Conference on Computer Vision*, IEEE. Kyoto, Japan: IEEE, Sept. 2009, pp. 2170–2176.

[7] C. Domokos, J. Nemeth, and Z. Kato, "Nonlinear shape registration without correspondences," *IEEE Transactions on Pattern Analysis and Machine Intelligence*, vol. 34, no. 5, pp. 943–958, May 2012.

[8] C. Domokos and Z. Kato, "Binary image registration using covariant Gaussian densities," in *International Conference on Image Analysis and Recognition*, ser. Lecture Notes in Computer Science, A. Campilho and M. Kamel, Eds., vol. 5112. Póvoa de Varzim, Portugal: Springer, June 2008, pp. 455–464.

[9] ——, "Affine alignment of compound objects: A direct approach," in *Proceedings of International Conference on Image Processing*, IEEE. Cairo, Egypt: IEEE, Nov. 2009, pp. 169–172.

[10] J. Nemeth, C. Domokos, and Z. Kato, "Nonlinear registration of binary shapes," in *Proceedings of International Conference on Image Processing*, IEEE. Cairo, Egypt: IEEE, Nov. 2009, pp. 1001–1004.

[11] C. Domokos, "Parametric estimation of affine deformations without correspondences," Ph.D. dissertation, University of Szeged, Szeged, Hungary, Sept. 2010.

[12] A. Tanacs, J. Lindblad, N. Sladoje, and Z. Kato, "Estimation of linear deformations of 2D and 3D fuzzy objects," *Pattern Recognition*, 2012, under review.

[13] C. Domokos and Z. Kato, "Affine shape alignment using covariant Gaussian densities: A direct solution," *Image and Vision Computing*, 2012, to be submitted.